Fast phase imaging in liquids using a rapid scan atomic force microscope

Takayuki Uchihashi[a] and Toshio Ando
Department of Physics, Kanazawa University, Kakuma-machi, Kanazawa 920-1192, Japan and Core Research for Evolutional Science and Technology (CREST) of the Japan Science and Technology Agency (JST), Kawaguchi, Saitama 332-0012, Japan

Hayato Yamashita
Department of Physics, Kanazawa University, Kakuma-machi, Kanazawa 920-1192, Japan

(Received 7 May 2006; accepted 4 October 2006; published online 22 November 2006)

The authors report on fast phase imaging in liquids achieved by fast phase detection in rapid scan atomic force microscopy. The phase-shift images clearly revealed the compositional heterogeneities in styrene-butadiene-styrene block copolymer films even at an imaging rate of less than 100 ms/frame. They found that the contrast variations of the phase images depended on the phase-shift detection timing within a single oscillation cycle. The phase contrast increased as the tip approached the surface in each oscillation during imaging, while it decreased as the tip withdrew from the surface. © *2006 American Institute of Physics*. [DOI: 10.1063/1.2387963]

Amplitude modulation atomic force microscopy (AFM)—referred to as tapping-mode AFM—has been established as a standard tool for the nanoscale imaging of the surfaces of various materials, particularly soft biological and polymer surfaces.[1–3] One of the significant features of tapping-mode AFM is its capability to image compositional variations in heterogeneous surfaces in addition to surface topography by detecting the phase difference between the exciting signal and the cantilever oscillation.[3–5] The phase shift is relevant to several surface properties such as viscoelasticity, elasticity, adhesion, hydrophobicity/hydrophilicity,[4] and surface charges.[6] The energy loss of an oscillating cantilever because of inelastic tip-sample interactions is considered to be the main mechanism of phase contrast.[7,8] On the other hand, efforts to improve the scan speed of AFM have led to an increase in its imaging rate.[9–11] High-speed AFM, particularly that based on tapping mode, performs more functions than contact-mode AFM. This is because it can be used to observe the dynamic processes of proteins.[10,12] Moreover, high-speed tapping-mode AFM can map dynamic material properties that accompany the structural changes in the sample.

To achieve fast phase imaging, the bandwidth for detecting the phase shift is required to be at least 70 kHz because in our present system, the feedback bandwidth is approximately 70 kHz. However, the bandwidth of a conventional lock-in amplifier is limited to dozens of kilohertz. In order to achieve fast phase detection, we have developed a fast phase detector based on a design by Stark and Guckemberger.[13] Figure 1 shows the working principle of fast phase detection. A two-channel wave form generator produces sinusoidal and sawtooth waves with a synchronized phase. The sinusoidal wave is used to oscillate the cantilever. The cantilever oscillation signal is fed to a phase detector composed of a high-pass filter, variable phase shifter, zero-crossing comparator, pulse generator, and sample-and-hold (S/H) circuit. A pulse signal is generated at either the rising or falling edge of the output signal of the zero-crossing comparator. The pulse signal serves as a trigger for the S/H circuit. At this trigger timing, the amplitude voltage of the sawtooth signal is retained by the S/H circuit. In Ref. 13, the usable resonant frequency of the cantilever is limited to 100 kHz because the sawtooth signal is reset for synchronization with the input signal. However, the use of the two-channel wave form generator allows us to use a cantilever with a much higher resonant frequency of over 1 MHz. In addition, the variable phase shifter enables us to vary the timing of the trigger signal generation within a cantilever oscillation cycle. This function is important to obtain the maximum phase contrast because the phase contrast can range from the not observable to the very large depending on the trigger timing as will be described later. By measuring the transient response of the output phase signal through a stepwise change in the phase of the sinusoidal input signal, the time constant τ was evaluated to be 0.12 μs, and the bandwidth was estimated to be 1.3 MHz, which is sufficiently higher than that of the feedback control of the high-speed AFM. The rms noise of the phase output signal is estimated to be about 3°.[14] It is known that the phase shift at the higher eigenmodes is significantly different from that at the fundamental frequency.[15,16] The fast phase detector does not discriminate the signals with different frequencies. However, the amplitude of the higher eigenmodes is usually less than 10% of the amplitude of the fundamental frequency. Therefore, the influence of the higher eigenmodes is considered to be negligible.

A block copolymer poly(styrene-butadiene-styrene) (SBS) was used as a test sample. SBS films are often used for phase imaging with tapping-mode AFM because the mechanical properties of glassy polystyrene (PS) and rubbery polybutadiene (PB) differ significantly.[3,17] The SBS copoly-

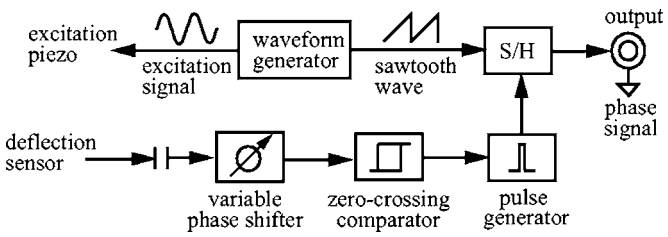

FIG. 1. Schematic diagram of the fast phase-detection system for AFM.

[a]Electronic mail: tuchi@kenroku.kanazawa-u.ac.jp

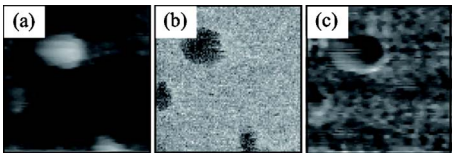

FIG. 2. (a) Topographic and (b) phase contrast images of a SBS film captured at 84 ms/frame in pure water. The scan area is 200 nm^2 with 100 $pixel^2$. The amplitude set point is 85% of the free amplitude of 13 nm_{p-p}. (c) Topographic image at the amplitude set point is reduced to 54%.

mer was prepared with a similar method described in Ref. 18. Before the AFM measurements, the sample was heated at 70 °C for 1 h. We used a home-built high-speed AFM, which is described in detail elsewhere.[10,12,19] The resonant frequency and quality factor of a cantilever in water were 658 kHz and approximately 2, respectively. Their spring constant was approximately 0.2 N/m.

Figure 2 shows typical (a) topographic and (b) phase images obtained simultaneously at 84 ms/frame in pure water. Here, phase detection was set to trigger when the tip approached the surface. We can obtain clear phase contrast images even at such a high imaging rate.[20] In the phase images, darker regions correspond to an advanced phase with an average shift of approximately 6° relative to the phase of brighter regions. To distinguish the compositions, the amplitude set point was reduced while imaging. The higher topographic region shown in Fig. 2(a) was suppressed by increasing the loading force, as shown in Fig. 2(c). The height was decreased by more than 5 nm. Hence, the major compositions in the higher and lower regions in Fig. 2(a) were considered to be less stiff PB and stiff PS domains, respectively.

To obtain the optimum phase contrast and an insight into the phase-shift mechanism, we investigated the dependence of phase contrasts on trigger timings. Figure 3(a) shows the signal of a cantilever oscillation measured in water. Figures 3(b)–3(d) show typical phase images obtained at various trigger timings. At the trigger points on the region indicated by (i) in Fig. 3(a), we observe only a faint phase contrast [Fig. 3(b)]. Since the image contrast of the error signal is similar to this phase contrast, the faint phase contrast is mainly due to the amplitude fluctuations. On the other hand, the phase image obtained at the trigger points on region (ii)

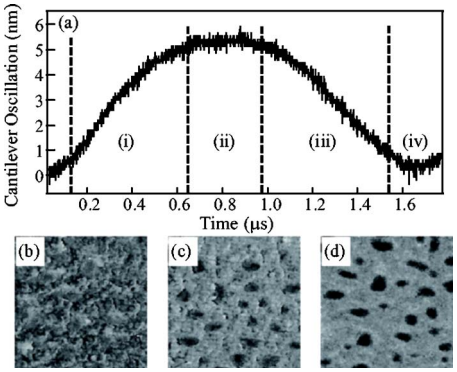

FIG. 3. (a) Cantilever oscillation signal and various trigger regions for phase detection. The amplitude set point is 63% of the free amplitude of 8.7 nm_{p-p}. The oscillation signal of "0 nm" corresponds to the distance where the tip is in contact with the surface. The phase contrast images shown in (b), (c), and (d) are obtained at trigger points within regions (i), (ii), and (iii), respectively. The imaging rate is 1.2 s/frame, and the scan area is 350 nm^2 with 200 $pixel^2$.

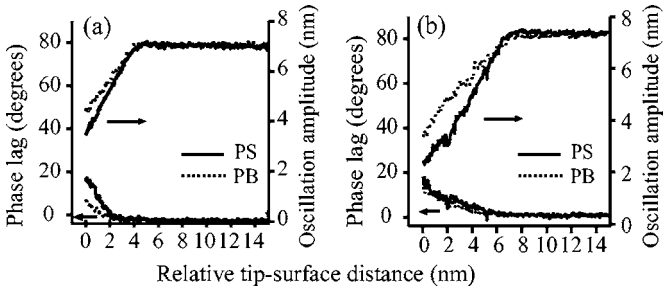

FIG. 4. Phase lags and antilever oscillation amplitudes as a function of the relative tip-surface distance measured on the trigger points in (a) region (iii) and in (b) region (i) shown in Fig. 3(a). Solid and dotted curves are obtained on PS and PB rich domains, respectively.

shows a relative phase advance of approximately 5° in the PB regions [Fig. 3(c)]. Then, at the trigger points on region (iii), we can clearly observe the phase contrast with a relative phase advance of approximately 10°, in the PB region [Fig. 3(d)]. The phase image obtained at the trigger points on region (iv) showed a similar contrast to that shown in Fig. 3(c). This result implies that the phase shift strongly depends on the trigger point; in other words, it depends on the direction of the movement of the oscillating tip. The largest phase shift is observed when the tip approaches the surface. However, when the tip withdraws from the surface, the phase shift hardly occurs. At the position where the tip velocity is almost zero, the phase shifts only slightly. Although we used three different cantilevers with resonant frequencies of about 600 kHz, 800 kHz, and 1.2 MHz, similar dependence was observed. In addition, the same result was observed, regardless of the scanning speed, free oscillating amplitude, and set-point amplitude.

Figures 4(a) and 4(b) show the phase lags and oscillation amplitudes as functions of the relative tip-surface distance recorded with different trigger timings. The decrease in the oscillation amplitude measured on the PS region is more significant than that measured on the PB region because the indentation on the soft PB region is larger than that on the stiff PS region, while the phase difference is only the delay for both the PS and PB regions. However, the phase lag on the PS region is larger than that on the PB region in Fig. 4(a), which forms an image contrast in the phase images, as shown in Figs. 2(b) and 3(d). On the other hand, the phase lags are almost similar on both the PS and PB regions in Fig. 4(b). In other words, the phase delay on the PS region is recovered at trigger points in region (i).

The phenomenon affecting the AFM phase image is complex because the phase difference depends on a number of instrumental and noninstrumental parameters.[3–8,21–24] Instrumental parameters such as the free oscillation amplitude and the set-point ratio affect the phase image contrast in a complex manner. It has been reported that a flipped phase contrast occurs when changing the tapping force level.[3,5,24] Such contrast flips generally occur due to the changes in the tip-sample interaction between the net attractive and repulsive force regimes.[25,26] However, we did not observe the phase contrast flips. In addition, the amplitude and phase curves obtained do not show the features of the transition from the "low-amplitude state" to the "high-amplitude state"[25] as shown in Figs. 4(a) and 4(b). Therefore, the tip-sample interaction is most likely a repulsive interaction (e.g., high oscillation amplitude state) for both the phase separated

regions under the present imaging conditions, in which the cantilever with a low quality factor is driven at the resonant frequency.[25] Under the repulsive force conditions, the phase contrast of a PS/PB blend film observed in an ambient condition mainly reflects the mechanical properties.[22,26] In this case, the phase signal is more delayed on the softer PB region rather than the harder PS region. This can be explained by the fact that the larger repulsive force on the harder material induces a positive resonant frequency shift, but the damping constants on both the materials are similar.[22,26] Such previous phase contrast does not coincide with our present result. Hence, the phase image contrast in the present study seems to have not originated from the variations in the mechanical properties between the PS and PB regions. Another possibility is the influence of the adhesion forces between the tip and the sample.[23,27] Although both PB and PS are nonpolar materials, PB is more polar than PS because a thermal treatment forms some C=O groups or other polar groups such as OH.[22] Since the AFM tip used here is composed of hydrophobic amorphous carbon, the adhesion forces would be larger on the PS region than on the PB region due to the hydrophobic interaction, which results in a larger phase delay on the PS region. In air, large capillary forces mask such chemical interactions,[23,27] but the mechanical properties are enhanced by a larger quality factor. In reality, we observed the phase contrast originating from the mechanical properties even by using the cantilever with a high resonant frequency of 2 MHz in air (data are not shown here).

The trigger timing dependence of the phase contrast might be explained by the damping of the cantilever oscillation in water that causes significant asymmetry on the sinusoidal oscillation due to damping in water. The phase delays occur on both the PS and PB regions, while on the harder PS region, a larger positive frequency shift occurs due to a larger repulsive force as compared to that on the PB region after the tip contacts the surface. Then, the positive frequency shift induces the phase advances at the fixed driving frequency. In liquid environment, the water medium damps the cantilever oscillation, and hence the phase advances are not kept within one oscillating cycle.[28] In other words, the phase of the oscillating tip advances just after the tip contacts the surface, but such phase advances become smaller with time. However, the phase delay is maintained over the oscillating cycle because the phase delay is caused by the dissipative adhesion forces. As a result, when the tip withdraws from the surface, the phase delay due to energy dissipation cancels the phase advance due to the increase in the repulsive force that causes a smaller phase lag on the PS region, as shown in Fig. 4(b). The dependence of the phase contrast on the trigger timing is not observed in air because the quality factor is relatively high; therefore, the distortion of the sinusoidal wave form decreases, and the phase advances on a harder material are maintained over an oscillating cycle. This would cause the enhancement of the mechanical properties in the phase image contrast under the ambient condition.

In summary, we developed the fast phase detector for high-speed tapping-mode AFM. It can detect the phase shift with a bandwidth of over 1 MHz. We succeeded in imaging both the topography and compositional heterogeneities in SBS films at 84 ms/frame in pure water. The main source of the phase contrast observed in the liquid is not so much the mechanical properties but the chemical properties. Furthermore, we found that the phase contrast strongly depends on the timing when the phase is detected within an oscillating cycle and is stronger when the tip approaches the surface. A combination of high-speed AFM and fast phase detection would enable us to study the dynamic changes in both the sample structures and physicochemical properties in the *in-liquid* tapping mode.

One of the authors (T.U.) was supported by an industrial technology research grant program in 2004 from NEDO and a Grant in Aid from the Ministry of Education, Culture, Sports, Science, and Technology, Japan.

[1] Q. Zhong, D. Innis, K. Kjoller, and V. B. Elings, Surf. Sci. Lett. **290**, L688 (1993).
[2] M. Radmacher, M. Fritz, and P. K. Hansma, Biophys. J. **69**, 264 (1995).
[3] S. N. Magonov, V. Elings, and M. H. Whangbo, Surf. Sci. **375**, L385 (1997).
[4] J. Tamayo and R. Garciá, Langmuir **12**, 4430 (1996).
[5] G. Bar, Y. Thomann, R. Brandsch, H. J. Cantow, and M. H. Whangbo, Langmuir **13**, 3807 (1997).
[6] D. M. Czajkowsky, M. J. Allen, V. Elings, and Z. Shao, Ultramicroscopy **74**, 1 (1998).
[7] J. P. Cleveland, B. Anczykowski, A. E. Schmid, and V. B. Elings, Appl. Phys. Lett. **72**, 2613 (1998).
[8] N. F. Martínez and R. Garciá, Nanotechnology **17**, S167 (2006).
[9] T. Sulchek, R. Hsieh, J. D. Adams, S. C. Minne, C. F. Quate, and D. M. Adderton, Rev. Sci. Instrum. **71**, 2097 (2000).
[10] T. Ando, N. Kodera, E. Takai, D. Maruyama, K. Saito, and A. Toda, Proc. Natl. Acad. Sci. U.S.A. **98**, 12468 (2001).
[11] A. D. L. Humphris, M. J. Miles, and J. K. Hobbs, Appl. Phys. Lett. **86**, 1 (2005).
[12] T. Ando, N. Kodera, T. Uchihashi, A. Miyagi, R. Nakakita, H. Yamashita, and K. Matada, e-J. Surf. Sci. Nanotechnol. **3**, 384 (2005).
[13] M. Stark and R. Guckenberger, Rev. Sci. Instrum. **70**, 3614 (1999).
[14] The rms noise can be reduced to less than 1° by using a low-pass filter with a bandwidth of a few hundred kilohertz, which is still sufficiently high.
[15] R. W. Stark, T. Drobek, and W. M. Heckl, Appl. Phys. Lett. **74**, 3296 (1999).
[16] R. W. Stark, G. Schitter, M. Stark, R. Guckenberger, and A. Stemmer, Phys. Rev. B **69**, 854121 (2004).
[17] R. Knoll, K. Magerle, and G. Krausch, Macromolecules **34**, 4159 (2001).
[18] Q. Zhang, O. K. C. Tsui, B. Du, F. Zhang, T. Tang, and T. He, Macromolecules **33**, 9561 (2000).
[19] T. Ando, N. Kodera, D. Maruyama, E. Takai, K. Saito, and A. Toda, Jpn. J. Appl. Phys., Part 1 **41**, 4851 (2002).
[20] Movies will be uploaded at our homepage (http://www.s.kanazawa-u. ac. jp/phys/biophys/index. htm).
[21] D. Raghavan, M. vanLandingham, X. Gu, and T. Nguyen, Langmuir **16**, 9448 (2000).
[22] D. Raghavan, X. Gu, T. Nguyen, M. vanLandingham, and A. Karim, Macromolecules **33**, 2573 (2000).
[23] A. Noy, C. H. Sanders, D. V. Vezenov, S. S. Wong, and C. M. Lieber, Langmuir **14**, 1508 (1998).
[24] B. B. Sauer, R. S. McLean, and R. R. Thomas, Langmuir **14**, 3045 (1998).
[25] R. W. Stark, G. Schitter, and A. Stemmer, Phys. Rev. B **68**, 854011 (2003).
[26] X. Chen, C. J. Roberts, J. Zhang, M. C. Davies, and S. J. B. Tendler, Surf. Sci. **519**, L593 (2002).
[27] M. Stark, C. Möller, D. J. Müller, and R. Guckenberger, Biophys. J. **80**, 3009 (2001).
[28] J. Legleiter and T. Kowalewski, Appl. Phys. Lett. **87**, 163120 (2005).